

Received 19 June 2025, accepted 1 July 2025, date of publication 7 July 2025, date of current version 15 July 2025.

Digital Object Identifier 10.1109/ACCESS.2025.3586246

RESEARCH ARTICLE

Integrating Immunotherapy With Targeted Therapy: Evaluating Efficacy in NSCLC Treatment Through Computational Analysis of Gene Regulatory Networks

PRANABESH BHATTACHARJEE¹, ADITYA LAHIRI¹, TANMAY SINDHWANI¹,
NORMAN PETER REEVES², AND ANIRUDDHA DATTA¹, (Fellow, IEEE)

¹Department of Electrical and Computer Engineering, Texas A&M University, College Station, TX 77843, USA

²Department of Biomedical and Health Informatics, The Children's Hospital of Philadelphia, Philadelphia, PA 19104, USA

³Sumaq Life LLC, Columbus, OH 43206, USA

Corresponding author: Pranabesh Bhattacharjee (p.bhattacharjee@tamu.edu)

This work was supported in part by the National Science Foundation under Grant ECCS-1917166.

ABSTRACT Non-Small Cell Lung Cancer (NSCLC) remains a leading cause of cancer-related deaths, often characterized by complex mutational landscapes and resistance to monotherapies. To address this, we developed a novel Boolean network (BN) model that integrates oncogenic and immunotherapy signaling pathways to evaluate the efficacy of FDA-approved drug combinations in NSCLC. This computational framework simulates the behavior of key cancer-related pathways under single and multiple mutation scenarios, offering a system-level understanding of drug response. Our model incorporates sixteen targeted inhibitors and simulates their effects on proliferation-promoting and apoptosis-regulating genes. Drug efficacy was quantitatively assessed using a normalized mean size difference (NMSD) metric. Unlike prior models that examine targeted therapy or immunotherapy in isolation, our integrated approach enables systematic evaluation of synergistic effects between these modalities. Key results show that the inclusion of immunotherapy—particularly PD-L1 inhibitors such as Durvalumab—significantly improves therapeutic outcomes, especially in networks with multiple co-occurring mutations. The most effective four-drug combination identified (Durvalumab + Lumakras + Ribociclib + Capivasertib) targets immune evasion, KRAS signaling, cell cycle regulation, and AKT activation, reducing tumor-promoting signals by 89.2% compared to the untreated state. This study provides a theoretical and mechanistic basis for combining immune checkpoint blockade with targeted therapies in NSCLC and demonstrates the utility of BN modeling in optimizing personalized, mutation-specific treatment strategies.

INDEX TERMS Boolean network, computational model, durvalumab, immunotherapy, lung cancer, NSCLC, PD-L1, signaling pathway, targeted therapy.

I. INTRODUCTION

Non-Small Cell Lung Cancer (NSCLC) constitutes the majority of lung cancer cases worldwide, contributing significantly to cancer-related morbidity and mortality. Globally, NSCLC accounted for approximately 80–85% of all lung cancer cases. There were 2,480,675 new cases of lung cancer in 2022

The associate editor coordinating the review of this manuscript and approving it for publication was Trung Q. Le¹.

[1], highlighting its pervasive impact. In the United States alone, NSCLC ranks as the second most common cancer. The American Cancer Society estimates that in 2024, there will be approximately 234,580 new cases of lung cancer in the US (116,310 in men and 118,270 in women). It also projects about 125,070 deaths from lung cancer (65,790 in men and 59,280 in women) [2], [3]. Despite significant advancements in targeted therapies and immunotherapy, achieving the best therapeutic outcomes in NSCLC remains challenging due to

the inherent heterogeneity and complexity of the disease [4], [5].

Survival rates for NSCLC vary significantly based on the stage at diagnosis, with localized NSCLC presenting a more favorable 5-year survival rate of approximately 63%, compared to 35% for regional spread and 8% for distant metastases [6]. This underscores the critical need for continued research and innovation in NSCLC treatment. Advances in understanding the molecular landscape of NSCLC and the development of robust computational models to predict treatment responses are pivotal in guiding personalized therapeutic approaches and improving patient outcomes [5], [7].

Treating NSCLC presents significant challenges, despite notable advancements in therapeutic options. One of the primary obstacles is the inherent heterogeneity of NSCLC, which includes various histological subtypes and genetic mutations [5], [8]. This diversity necessitates personalized treatment approaches tailored to individual patient profiles, which adds complexity to clinical decision-making [9]. Personalized medicine has emerged as a promising strategy to enhance treatment efficacy by tailoring therapies to individual patient characteristics [10]. This approach requires a comprehensive understanding of the disease's molecular underpinnings, which advancements in genomic and computational technologies have greatly aided [5], [7].

Targeted therapies directed at specific genetic alterations, such as Epidermal Growth Factor Receptor (EGFR) mutations and Anaplastic Lymphoma Kinase (ALK) rearrangements, have demonstrated good efficacy in the treatment of NSCLC [11]. However, challenges such as acquired resistance to targeted therapies and the identification of the best possible treatment strategies for diverse patient populations continue to persist [12], [13]. Continued research is essential to fully understand and overcome these mechanisms of resistance, paving the way for more durable and effective treatment strategies in NSCLC [13]. Additionally, late diagnosis often occurs in NSCLC cases, leading to advanced stages at presentation and limiting treatment effectiveness [14]. For patients with advanced disease, treatment options may be further constrained, highlighting the need for expanded therapeutic strategies. Moreover, the toxicity associated with current treatments, particularly chemotherapy, poses challenges in managing patient symptoms and maintaining treatment adherence. While immunotherapy generally has lower toxicity, it still presents certain challenges that must be carefully managed [15], [16]. Cost and accessibility issues also impact treatment decisions, with novel therapies often being expensive and not universally available. Lastly, limited access to clinical trials hinders the exploration of new treatment modalities and combinations, particularly for underserved populations [17]. Addressing these challenges requires continued research into NSCLC biology, advancements in precision medicine approaches [5], improvements in early detection methods, and efforts to ensure equitable

access to effective treatments for all NSCLC patients. Traditional targeted therapies, though promising, often fall short due to the genetic heterogeneity and adaptive resistance mechanisms of NSCLC tumors [13], [18], [19]. The advent of immunotherapies, particularly those targeting the PD-1/PD-L1 pathway, has shown significant potential in enhancing anti-tumor responses [16], [20], [21].

Motivated by these considerations, we used a Boolean network (BN) [22], [23] to model the pathways and identify the best possible drug targets and thereby identify the best drug combinations [24], [26], [27], for NSCLC treatment by integrating targeted therapy and immunotherapy pathways. BNs are computational models that simplify gene behavior by representing each gene's regulatory state as either 'on' (upregulated) or 'off' (downregulated). This helps researchers study how genes interact with each other and identify key genes that could be potential drug targets. In recent years, the use of such models has proven to be an effective tool for simulating and analyzing the intricate signaling pathways involved in the progression of various cancers [7], [28], [29], [31]. This research evaluates the efficacy of combining targeted therapy with immunotherapy in controlling specific genes within the NSCLC pathway using a BN model. By integrating the PD-L1/PD1 immunotherapy pathway into our BN model, we can assess the synergistic effects of these therapies. The PD-L1/PD1 pathway, known for its significant clinical outcomes, is crucial in enhancing the overall effectiveness of the NSCLC treatment regimen [16], [32].

Computational modeling of cancer treatment responses faces several significant challenges [7], [8], [10], [11], [19], [20], [31], including capturing the complexity of cellular signaling networks, accounting for genetic heterogeneity among tumors, and integrating diverse treatment modalities with distinct mechanisms of action. Previous computational approaches have typically focused on either targeted therapy affecting specific oncogenic pathways or immunotherapies modulating immune responses, but rarely both simultaneously [6], [7], [20]. Additionally, most models struggle to translate theoretical predictions into clinically actionable insights due to their complexity or reliance on parameters that cannot be easily measured [8]. Our research addresses these challenges by developing an integrated Boolean network model that combines both treatment modalities and produces predictions directly relating to FDA-approved therapies.

The paper is organized as follows. In Section II, we describe the molecular pathways and key proteins involved in the progression of NSCLC. Section III presents the computational methodology for analyzing the abnormalities and therapeutic interventions for the NSCLC signaling pathways. In Section IV, we present the results in terms of the predicted efficacy of different drug combinations. Section V concludes the paper by summarizing the main results and outlining the topics for future research.

II. MOLECULAR PATHWAYS AND KEY PROTEINS IN NSCLC PROGRESSION

Cells perform essential functions such as metabolism and differentiation through signaling pathways. These pathways consist of various molecules, including proteins, genes, and transcription factors, that work together in a coordinated manner to perform specific cellular functions [32]. Signaling pathways in cells are activated by stimuli or signaling molecules such as hormones or growth factors that bind to specialized proteins called receptors on the cell surface. These receptors then activate downstream molecules, initiating a cascade of intracellular signaling activities. This signaling continues until the final molecule in the pathway is activated. Disruptions in signaling pathways or abnormal activation/inhibition due to genetic mutations can lead to aberrant signaling behavior, resulting in the loss of cell cycle control and potentially causing cancer [33]. Understanding the key proteins and pathways involved in NSCLC progression is crucial for developing targeted therapies and improving patient outcomes. This section delineates the roles of critical pathways implicated in NSCLC, their interactions, and their contributions to tumorigenesis. Our goal was to adopt a system-level approach to examine the impact of mutations on entire signaling pathways, rather than focusing solely on the nature of the genetic mutations, and a brief description of each pathway (associated with NSCLC) follows.

A. EGFR PATHWAY

EGFR (Epidermal Growth Factor Receptor) is a transmembrane receptor tyrosine kinase that, upon activation by ligands such as Epidermal Growth Factor (EGF) and Transforming Growth Factor-alpha (TGF- α), triggers a series of downstream signaling pathways. These pathways include the RAS-RAF-MEK-ERK and PI3K-AKT cascades, which collectively promote cell proliferation, survival, and differentiation [34]. The activation process starts with the binding of EGF or TGF- α to EGFR, resulting in receptor dimerization and subsequent autophosphorylation of tyrosine residues [35]. In NSCLC, EGFR mutations or overexpression often led to dysregulated cell growth. To address this, targeted therapies such as Osimertinib, a tyrosine kinase inhibitor (TKI) [36], [37], have been developed to specifically inhibit the aberrant EGFR signaling pathways.

B. ERBB2 PATHWAY

ERBB2 is also known as Human Epidermal Growth Factor Receptor 2 (HER2) and is another member of the EGFR family. It is a receptor tyrosine kinase (belonging to the ErbB family of receptor tyrosine kinases) and is involved in cell growth, differentiation, and survival, and is often amplified in NSCLC [38], [39]. Ligand binding to partner receptors (EGFR) leads to dimerization with ERBB2, resulting in autophosphorylation and activation of its kinase domain. Its overexpression results in enhanced dimerization and activation of downstream signaling pathways, particularly the

PI3K/AKT, PLC γ -PKC, and MAPK pathways, contributing to increased cell proliferation and tumor growth [40]. Anti-ERBB2 therapies, such as Trastuzumab-Deruxtecan, have shown efficacy in targeting ERBB2-positive cancers [41].

C. ALK PATHWAY

ALK (Anaplastic Lymphoma Kinase) is a receptor tyrosine kinase involved in cell growth and differentiation [42]. The EML4-ALK fusion protein results from chromosomal rearrangement and acts as a constitutively active tyrosine kinase, driving oncogenic signaling like MAPK, PI3K-AKT, and JAK-STAT [42]. This fusion is a hallmark of a subset of NSCLC and is targeted by ALK inhibitors such as Lorlatinib, which have demonstrated significant clinical efficacy [43].

D. KRAS PATHWAY

KRAS (Kirsten Rat Sarcoma Viral Oncogene Homolog) is a small GTPase that acts as a molecular switch in signaling pathways controlling cell growth and survival [44]. KRAS mutations are prevalent in NSCLC and result in the constitutive activation of the MAPK signaling pathway [44], promoting cell proliferation and survival. Direct targeting of mutant KRAS has been challenging, but recent developments like the KRAS G12C inhibitor: Sotorasib (Lumakras) offer promising therapeutic options [45].

E. PI3K/AKT/mTOR PATHWAY

The PI3K/AKT/mTOR pathway is crucial for regulating cell growth, proliferation, and survival. Activation is triggered by receptor tyrosine kinases (e.g., EGFR) and G-protein-coupled receptors [35]. PI3K (Phosphatidylinositol 3-kinase) activation leads to the production of Phosphatidylinositol (3,4,5)-trisphosphate (PIP3), which recruits and activates Protein kinase B (PKB/AKT). AKT phosphorylation targets are involved in cell growth and survival (e.g., mTOR, BAD) [46]. PTEN (Phosphatase and Tensin Homolog) is a tumor suppressor that negatively regulates the PI3K/AKT pathway [46]. Loss of PTEN function, through mutations or deletions, leads to hyperactivation of the PI3K/AKT pathway, contributing to tumorigenesis by promoting cell survival and proliferation. Dysregulation of this pathway, through mutations in PI3K or loss of PTEN, is common in NSCLC. Inhibitors targeting various components of this pathway, such as Alpelisib (PI3K inhibitor) and Everolimus (mTOR inhibitor), are being explored for their therapeutic potential [47].

F. JAK/STAT PATHWAY

Activation of the JAK/STAT (Janus kinase/signal transducer and activator of transcription) pathway, particularly STAT3, is implicated in NSCLC progression [48]. Constitutive activation of STAT3 promotes cell survival, proliferation, and immune evasion. Targeting the JAK/STAT pathway, either through direct STAT3 inhibitors or JAK inhibitors [48], represents a therapeutic strategy to counteract its oncogenic

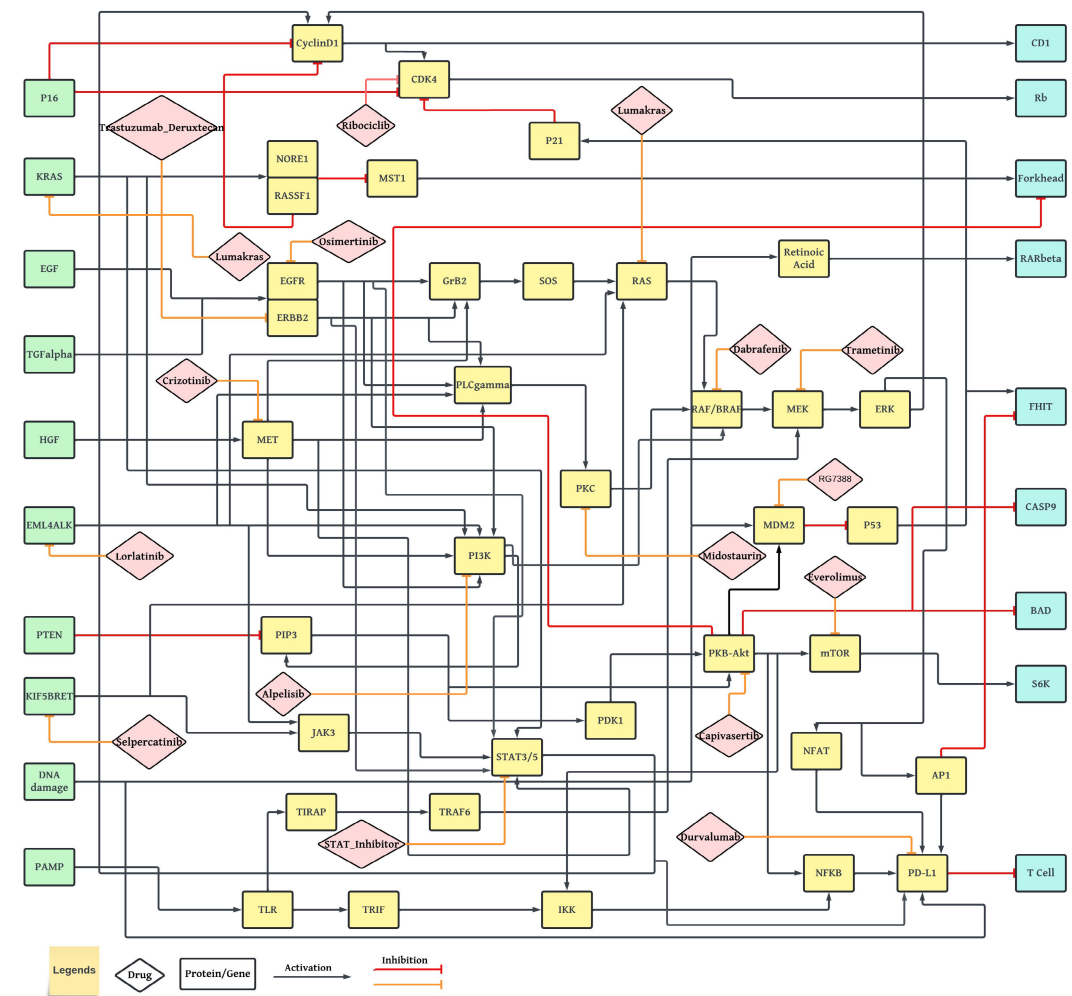


FIGURE 1. NSCLC signaling pathway with all drugs intervention points.

effects. Currently, there are no available FDA-approved drugs for treating STAT mutations.

G. MAPK PATHWAY

The MAPK (Mitogen-Activated Protein Kinase) pathway controls cell growth, differentiation, and survival. Activation is triggered by growth factors binding to receptor tyrosine kinases. Downstream, it involves sequential activation of RAS (rat sarcoma virus protein), RAF (Rapidly Accelerated Fibrosarcoma), MEK (Mitogen-activated protein kinase kinase), and ERK (Extracellular signal-regulated kinase) [49]. Mutations in components of this pathway (e.g., RAS, RAF) lead to uncontrolled proliferation [50]. The MET (Mesenchymal-Epithelial Transition factor) is a proto-oncogene that encodes the MET receptor tyrosine kinase. The MET receptor and its ligand, hepatocyte growth factor (HGF), play crucial roles in various cellular processes, including growth, survival, angiogenesis, and metastasis. In NSCLC, MET amplification or mutations lead to constitutive activation of downstream signaling, like MAPK,

PI3K-AKT, RAS, and JAK/STAT pathways promoting tumor growth and metastasis [45]. Inhibitors like Crizotinib target the aberrant MET signaling in NSCLC [51].

H. DDR PATHWAY

The DDR (DNA Damage Response) pathway plays a crucial role in maintaining genomic integrity and preventing mutations that can lead to cancer. In NSCLC, key proteins such as MDM2 (Murine Double Minute 2), PD-L1 (Programmed Cell Death Ligand 1), and retinoic acid are significant components of this pathway. MDM2 is an E3 ubiquitin ligase that negatively regulates the tumor suppressor p53, thereby influencing cell cycle progression and apoptosis in response to DNA damage. The overexpression of MDM2 in NSCLC can compromise the cell's ability to induce cell cycle arrest and apoptosis, promoting tumor progression [52]. Targeting these components—MDM2, PD-L1, and retinoic acid—can provide a multifaceted approach to improve treatment efficacy in NSCLC by addressing both the repair of DNA damage and the immune evasion strategies employed by tumors.

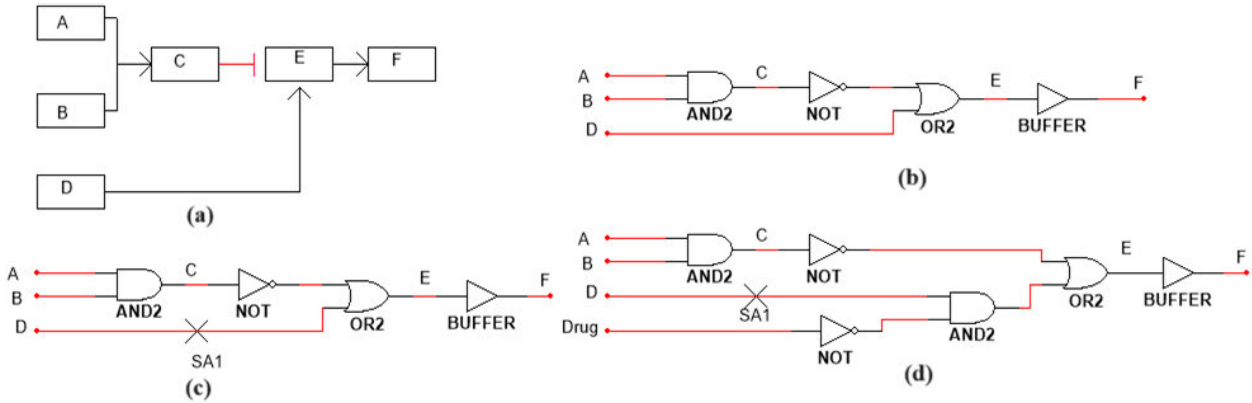


FIGURE 2. (a) Example of a signaling pathway. (b) BN model example of the signaling pathway. (c) BN with a stuck-at-1 (SA1) fault at gene D. (d) BN with drug intervention at gene D to repair the SA1 fault.

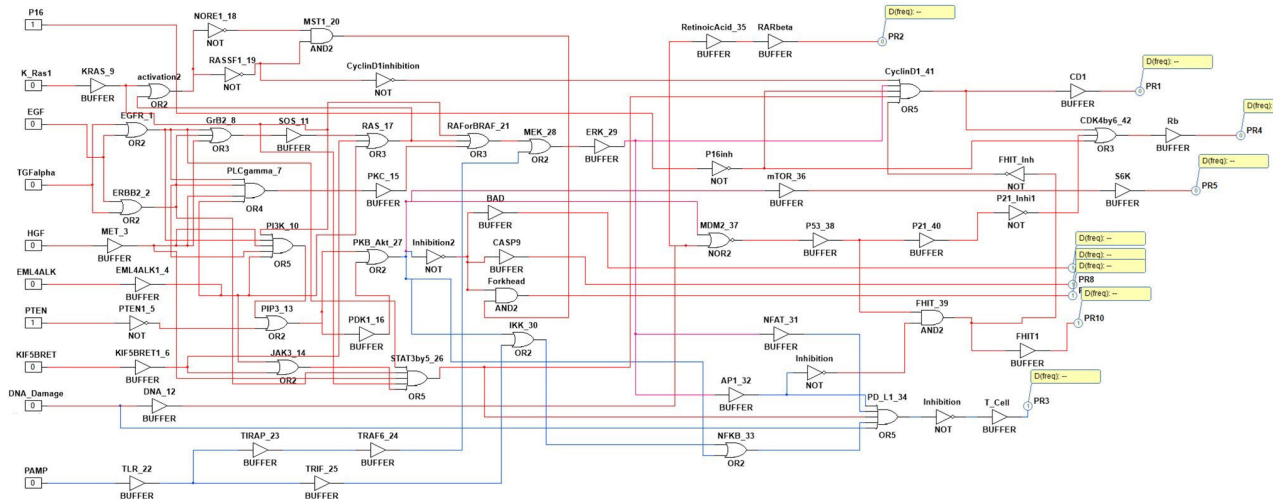


FIGURE 3. Boolean Network model for NSCLC pathway with PDL1, this diagram also shows its ideal input and output states.

I. ITP53 PATHWAY

p53 (Tumor Protein p53) is a tumor suppressor protein that regulates the cell cycle and apoptosis. Activated by cellular stress or DNA damage, it induces cell cycle arrest, DNA repair, and apoptosis [52]. MDM2, a negative regulator of p53, inhibits its activity by promoting its ubiquitination and degradation. This interaction is crucial because it prevents p53 from accumulating in cells under normal conditions. However, in response to stress, the p53-MDM2 interaction is disrupted, allowing p53 to activate its target genes. TP53 is the name of the gene, while p53 is the name of the protein that the gene encodes. TP53 mutations are common in NSCLC, leading to loss of tumor suppressor function and contributing to tumor progression. [53].

J. PD-L1 PATHWAY

PD-L1 (Programmed Death-Ligand 1) expression on tumor cells interacts with PD-1 on T cells, leading to immune evasion. High PD-L1 expression is associated with poor

prognosis in NSCLC [52]. PD-L1 is a critical immune checkpoint protein that can be upregulated in response to various stress signals, including DNA damage. Its expression allows cancer cells to evade immune surveillance, making it a target for immunotherapy. The interplay between PD-L1 and the DDR pathway highlights the importance of targeting immune evasion mechanisms in conjunction with DNA repair processes. Immune checkpoint inhibitors, such as Durvalumab, block the PD-1/PD-L1 interaction, reactivating the immune response against tumor cells and improving patient outcomes [54].

The progression of NSCLC is driven by a complex interplay of oncogenes, tumor suppressors, and signaling pathways. Key proteins such as EGFR, ERBB2, MET, EML4-ALK, PTEN, KRAS, p53, and components of the PI3K/AKT/mTOR and JAK/STAT pathways play critical roles in tumorigenesis. Understanding these molecular mechanisms has led to the development of targeted therapies, which are transforming the treatment landscape of NSCLC.

III. METHODOLOGY FOR ANALYSIS OF GENE MUTATIONS IN THE NSCLC PATHWAY

This paper aims to computationally predict the effects of different combinations of FDA approved drugs on the NSCLC pathway under the presence of genetic mutations. We achieve this by simulating the effect of combinations of multiple drugs on the pathway under various combinations of genetic mutations and calculating the efficacy of each drug combination in maximizing cancer cell death and minimizing their proliferation, as quantified by an efficacy metric known as the normalized mean size difference (NMSD) which is defined later in the paper. Ranking the drug combinations in terms of NMSD allows us to determine which pathway elements serve as potential drug targets. The details of our methodology are described in the following subsections A-F.

A. DEFINE THE NSCLC PATHWAY AND PROTEINS

For this study, we focused on a network of 42 proteins and genes (Fig. 1) to understand their interconnections and interactions in the progress of NSCLC. These proteins are part of a gene regulatory network (GRN). GRNs are used to represent the complex interactions between genes, proteins, and other molecular components that govern biological processes. In NSCLC, the GRN includes key players such as EML4-ALK, KRAS, etc. which interact within various signaling pathways mentioned in the last section, to influence tumorigenesis, proliferation, and apoptosis [55]. Understanding these complex interconnections within the GRN is essential for developing targeted therapies that can effectively address the unique molecular characteristics of NSCLC and improve patient outcomes. By studying these interactions, we aim to uncover the underlying mechanisms of diseases that occur when mutations disrupt normal cellular processes.

Figure 1 provides a comprehensive visualization of the integrated NSCLC signaling pathway with all potential drug intervention points highlighted. The network illustrates the complex interconnections between key oncogenic pathways, including EGFR, PI3K/AKT/mTOR, MAPK, and PD-L1/PD-1 signaling. Green nodes represent growth factors and receptors that initiate signaling cascades. Blue nodes represent reporter genes and cell cycle regulators that control apoptosis and proliferation. Yellow nodes highlight all other genes and proteins that participate in disease progression. Purple diamond-shaped nodes mark the 16 drug intervention points explored in our study, demonstrating how targeted therapies and immunotherapies can modulate different aspects of the network. Solid lines with arrows indicate activating interactions, while solid lines ending with a hammer represent inhibitory relationships. This comprehensive pathway diagram serves as the foundation for our Boolean network model, capturing the essential regulatory relationships that drive NSCLC progression and treatment response.

B. MODELING THE SIGNALING PATHWAY WITH BOOLEAN NETWORKS

A key aspect of GRNs is their ability to model the regulatory mechanisms underlying signaling pathways. To study these pathways, different computational modeling approaches have been developed. One widely used approach is the BN model, which provides a simplified representation of GRNs by focusing on the binary states of gene activation or inactivation [57], [58], [59].

In a BN modeling approach, each gene or regulatory element is represented as a node that can exist in one of two states: active (2) or inactive (0) (Fig. 2). These binary states can approximate the up-regulation or down-regulation of gene expression levels observed in GRNs. The BN model captures the interactions and dependencies between genes, providing insights into their dynamic behavior. By applying BNs to model GRNs, researchers can explore how various genes interact and regulate each other in response to different signals, thereby gaining a better understanding of complex biological networks. This switch-like behavior of many genes can be effectively modeled within a binary framework, making BN a suitable choice for modeling GRNs. Furthermore, in a GRN, a gene is influenced by one or more other genes. This interaction among genes can be modeled as a Boolean logic function.

Modeling gene regulatory networks using BN was first introduced in 1969 [60], [61], [62]. Formally, a BN consists of a collection of binary-valued variables $X = \{x_1, x_2, x_3, \dots, x_n\}$ and a set of Boolean functions $F = \{f_1, f_2, f_3, \dots, f_n\}$ [63], [64]. BN can also be represented as a directed graph G , where the elements of X represent nodes or system variables, connected by directed edges [64]. These nodes are binary-valued, indicating they can be either inactive (0) or active (2). The causal interactions between nodes are described by the Boolean functions in F [64]. In the context of signaling pathways, elements such as genes and transcription factors can be upregulated (activated) or downregulated (inhibited), and this behavior can be modeled using the binary framework of BNs. We provide an example of BN modeling using a simple signaling pathway in Fig. 2.

In Fig. 2(a), we present a signaling pathway composed of six genes (A-F). When genes A and B are upregulated, they bind together to activate gene C. Activated gene C inhibits gene E, while gene D activates gene E. Subsequently, activated gene E activates gene F. In this example, we model these genes using BN by considering them as either activated (upregulated) or inhibited (downregulated). Fig. 2(b) illustrates the BN equivalent of the pathway shown in Fig. 2(a). Since both genes A and B must be activated to turn on gene C, this relationship is modeled using a logical AND gate, represented by the Boolean function $C = A \& B$. Gene C inhibits gene E; hence, the signal from gene C to gene E first passes through a NOT gate. This signal then combines with the input signal from gene D via an OR gate to regulate gene E. Therefore, the Boolean function for gene E is $E = (\sim C) | D$.

TABLE 1. Inputs of the NSCLC boolean network (without faults) and their corresponding non-proliferative states.

Input	Non-Proliferative Input State
P16	1
KRAS	0
EGF	0
TGF_alpha	0
HGF	0
EM4ALK	0
PTEN	1
KIF5BRET	0
DNA_Damage	0
PAMP	0

Gene E activates gene F, and this interaction is represented using a follower or buffer, with the Boolean function for gene F given by $F = E$.

C. MODELING ABNORMALITIES IN THE BOOLEAN NETWORK

Cancerous mutations in genes can cause a gene to be permanently up-regulated or down-regulated, resulting in abnormal or faulty signaling. When such a mutation occurs in a gene then it is no longer influenced by the activity of other genes. Such permanent up-regulation or down-regulation could be modeled as a stuck-at-fault (0 or 1) in the BN model. A gene stuck at state '0' indicates that the gene is inactive, while a gene stuck at '1' signifies that the gene is active. Thus, if a cancerous mutation causes the gene to become upregulated/active, then we model this mutation with a stuck-at-1 (SA1) fault and if the mutated gene becomes downregulated/inactive then we model it as a stuck-at-0 (SA0) fault. An example of a stuck-at-1 fault is shown in the toy signaling model in Fig. 2(c).

The NSCLC BN model in this study has 10 inputs, which include growth factors, and tumor suppressors, and its 9 outputs are reporter genes (Fig. 3). Therefore, the input and output vectors for our NSCLC pathway diagram can be represented as follows:

Input = [P16, KRAS, EGF, TGF α , HGF, EML4ALK, PTEN, KIF5BRET, DNA_Damage, PAMP]

Output = [RARbeta, CD1, Rb, S6K, BAD, CASP9, Forkhead, FHIT1, T_Cell]

Figure 3 presents our complete Boolean Network model for the NSCLC pathway, integrating the PD-L1 immune checkpoint pathway with traditional oncogenic signaling. The diagram illustrates the logical architecture of the network, comprising 42 nodes (genes/proteins) interconnected through logical operations (AND, OR, NOT and Buffer) that represent their regulatory relationships. Input nodes (depicted on the left) include growth factors (EGF, TGF- α , HGF), oncogenes (KRAS, EML4-ALK, KIF5BRET), tumor suppressors (P16, PTEN), and immune stimuli (PAMP, DNA_Damage). Output nodes (shown on the right) represent critical cellular processes and include proliferation markers (CD1, Rb, S6K), apoptosis regulators (BAD, CASP9, Forkhead), tumor suppressors (FHIT1, RARbeta), and immune response indicators

TABLE 2. Outputs of the NSCLC boolean network (without faults) and their corresponding non-proliferative states.

Output	Non-Proliferative Output State
RARbeta	0
CD1	0
Rb	0
S6K	0
BAD	1
CASP9	1
Forkhead	1
FHIT1	1
T_Cell	1

(T_Cell). The non-proliferative input state of the pathway diagram is shown below the input nodes, where tumor suppressors are activated (1) and oncogenic signals are deactivated (0). Likewise, the ideal output state is indicated below the output nodes, with cancer-promoting genes turned off (0), and tumor-suppressive, apoptotic, or immune-response genes turned on (1). This model structure allows us to simulate the effects of mutations (represented as stuck-at faults) and drug interventions on the system's behavior, enabling quantitative assessment of treatment efficacy. For this BN model, the ideal test input state is defined as when the proliferative inputs such as the growth factors are turned off and the tumor suppressors are turned on. Thus, the non-proliferative test input and consequently the non-proliferative output (when there are no gene mutations in the pathway) are defined as follows:

$$\text{Ideal Input} = [1, 0, 0, 0, 0, 0, 1, 0, 0, 0]$$

$$\text{Ideal Output} = [0, 0, 0, 1, 1, 1, 1, 1]$$

We define the non-proliferative input/output states in this manner because, for a healthy cell, a non-proliferative input state implies that the tumor suppressors PTEN and P16 are activated (state 1). In contrast, the other proliferative inputs are deactivated (state 0). Thus, the corresponding fault-free output must have all cancer-promoting reporter genes turned off and all cancer-suppressing genes such as the pro-apoptotic genes turned on. This condition can be verified in the mutation (fault)-free network shown in Fig. 3, where the inputs are in an ideal state, which means all the growth factors are turned off and all the tumor suppressor genes are turned on. Boolean logic 1 and 0 were used in our BN model (Fig. 3) to define these On and Off conditions respectively. The non proliferative input and its corresponding output state for the fault-free BN depicted in Fig. 3 are displayed in Tables 1 and 2, respectively.

To evaluate drug efficacies, we considered that multiple faults could occur simultaneously in the network, meaning the NSCLC pathway can have more than one mutation at a time. Due to computational complexity, we limited our study to a maximum of three faults (mutations) occurring at a time in BN. With 42 individual faults, we evaluated drug efficacies across $4^2 C_1 + 4^2 C_2 + 4^2 C_3 = 12383$ combinations of faults. The three terms in the above summation enumerate all the possible combinations of 42 mutations that can occur when we restrict ourselves to a maximum of three simultaneously

TABLE 3. List of all drugs and corresponding targets [25], [26], [27].

Drugs	Targets
Osimertinib	EGFR
Selpercatinib	KIF5B-RET
Trastuzumab_Deruxtecan	ERBB2
Crizotinib	MET
Dabrafenib	RAF
Durvalumab	PD-L1
Trametinib	MEK
Alpelisib	PI3K
Midostaurin	PKC
Lumakras	KRAS
RG7388	MDM2
Ribociclib	CDK4/6
STAT_Inhibitor	STAT3/5
Everolimus	mTOR
Lorlatinib	EML4-ALK
Capivasertib	AKT

occurring mutations. The two and three-fault scenarios are the cases when two and three mutations occur across any of the 42 possible genes in the signaling pathway. We consider all the possible combinations of two and three faults that can occur across the 42 fault locations (${}^{42}C_2$, ${}^{42}C_3$) and simulate the effect of each drug combination on these combinations of mutations using the BN model.

D. DRUG SELECTION AND MODELING DRUG INTERVENTION

Drugs typically exert their effects by interacting with receptors on the cell surface or enzymes within cells. They can either inhibit (block) or enhance (induce) the function of a protein by binding to its target receptor site. This drug interaction can be represented in a BN by either forcibly suppressing or enhancing the value of a gene at the appropriate location.

To illustrate this type of modeling, we return to our earlier toy example Fig. 2(d) illustrates the application of a drug that inhibits its target molecule, gene D. In the BN, this interaction is represented by a NOT gate (inhibition) followed by an AND gate (binding). We considered gene D as a faulty gene that is unexpectedly always turned on and stuck at a value of '1' (Fig. 2(c)) which means that whatever the value of gene C is, it is not at all controlling the state of gene E or F as it is supposed to. When we use an inhibitory drug at D at state 1 (which means the drug is present or active), it sends an inhibitory signal (0) to gene D (Fig. 2(d)). Gene E not only receives a signal from gene D but also from gene C, meaning both gene C and gene D, with the effect of the inhibitory drug incorporated, influence gene E, which is modeled using an AND gate. Because the AND gate receives an inhibitory signal (0) from the drug, it successfully inhibits gene D. Recall that in our Boolean gene regulatory network modeling approach, whenever a protein binds with another protein, we model it using an AND gate. A similar modeling is shown for the drug because, in practical applications, the drug binds with the targeted protein. It should be noted that, in the presence of the drug, the mutation in gene D, represented by

a stuck-at-1 fault, can no longer influence the state of gene E or its upregulated gene F.

In this study, we evaluate the effect of 16 different small-molecule inhibitory drugs (Table 3) on an NSCLC signaling pathway with mutations. We considered a total of 42 unique mutation locations. The objective was to determine how effective these drugs were in mitigating the aberrant behavior caused by mutations in the NSCLC network. Table 3 outlines the sixteen drugs and their molecular targets. We focus on targets rather than specific drugs, as this study is computational, leaving the selection of specific drugs to clinicians. Furthermore, it is possible that certain drug targets don't currently have any approved medications accessible, and our approach can highlight the potential value of designing new drugs for these targets. For example, in Table 3 we indicated a STAT Inhibitor to target STAT3/5 because there is no FDA-approved drug in the market that targets it. For the 16 drugs considered here, we assign the value '1' when the corresponding drug is being used and '0' when it is not being used.

E. GENERATE DRUG COMBINATIONS

In addition to the 16 drugs, which can be administered individually, we also evaluate the results of using drug combinations. Due to computational complexity and the potential adverse effects of administering too many drugs simultaneously, we limit our study to a maximum of 4 drugs applied at once. For each drug or drug combination, we determine its drug-induced output across each of the 12,383 fault combinations and then compare the drug-induced output to the non-proliferative output.

We used combinatorial techniques to generate all possible combinations of the drugs mentioned in Table 3. Since there are 16 drugs and we considered combinations of up to four drugs at a time, this results in a total of ${}^{16}C_1 + {}^{16}C_2 + {}^{16}C_3 + {}^{16}C_4 = 2516$ drug combinations. The Boolean network was then simulated with these drug combinations in the presence of one, two, or three faults (mutations).

F. COMPUTE THE EFFECTS OF DRUG COMBINATIONS

For each drug combination, we computed the effect of introducing one, two, or three mutations in the pathway. From a system-level perspective, the Boolean network (BN) representing NSCLC is analogous to a multi-input multi-output (MIMO) digital circuit. In the absence of faults or mutations, the output of the system is determined solely by its inputs. Thus, a fault-free network receiving non-proliferative input signals accurately reflects the signaling behavior of a healthy cell. In contrast, if the same non-proliferative inputs are applied to a BN with faults (e.g., mutations), the network produces a different output, representing the aberrant signaling typical of cancerous cells. This divergence in output highlights that cancerous cells do not share the same input-output mapping as healthy cells. Therefore, when a non-proliferative signal is applied in the presence of mutations, the resulting output deviates from the expected healthy

TABLE 4. A sample NMSD chart.

	Fault 1	Fault 2	Fault 3	NMSD
Drug 1	0.3	0.4	0.7	0.609
Drug 2	0.1	0.5	0.2	0.348
Drug 3	0.5	0.3	0.4	0.522
Untreated	0.6	0.8	0.9	1.000

state, illustrating the impact of dysregulated signaling in cancer. Therefore, administering drugs to a network with faults has the potential to drive the output towards a non-proliferative state. To measure the efficacy of each drug, it is essential to assess how much the drugged output differs from the non-proliferative output state. To quantitatively measure this difference between the outputs (it must be noted that the outputs of a BN are binary-valued vectors) we used the size difference (SD) score. SD measures the difference between two binary-valued vectors, with its value increasing proportionally with greater dissimilarity.

To mathematically describe SD, we have taken two binary (0 or 1) valued vectors $a = (a_1, \dots, a_n)$ and $b = (b_1, \dots, b_n)$, where n represents the size of the vectors [64]. Then, we can construct a confusion matrix M as follows:

$$M = \begin{matrix} & \begin{matrix} a_i = 1 & a_i = 0 \end{matrix} \\ \begin{matrix} b_i = 1 \\ b_i = 0 \end{matrix} & \begin{pmatrix} A & B \\ C & D \end{pmatrix} \end{matrix} \quad (1)$$

Equation 1 introduces the confusion matrix M , which serves as a fundamental tool for comparing binary vectors in our Boolean network analysis. This matrix categorizes each element comparison into one of four possible outcomes: when both elements are 1 (A), when only the second element is 1 (B), when only the first element is 1 (C), or when both elements are 0 (D). This classification enables us to quantify both the matches (A and D) and mismatches (B and C) between the vectors, providing a mathematical foundation for measuring the difference between non-proliferative and proliferative states in our network. Therefore, with the help of the confusion matrix M (Refer to “(1)”), we define SD as follows:

$$SD(a, b) = \left(\frac{B + C}{A + B + C + D} \right)^2, \quad SD \in [0, 1] \quad (2)$$

Equation 2 defines the SD metric, which quantifies the dissimilarity between two binary vectors. This metric is particularly well-suited for our Boolean network analysis as it normalizes the count of mismatches ($B+C$) by the total number of comparisons ($A+B+C+D$), then squares this ratio to yield a value between 0 and 1. The squaring operation emphasizes larger differences and de-emphasizes smaller ones, making SD more sensitive to significant deviations from the non-proliferative state. A value of 0 indicates identical vectors (perfect match to non-proliferative state), while 1 indicates that one vector is the binary complement of the other (maximum deviation from non-proliferative state).

This metric provides a crucial quantitative basis for evaluating how effectively different drug combinations restore the output of the mutated network towards a non-proliferative state. In our fault-free BN, the state of the non-proliferative output requires all output genes to be in the state mentioned in Table 2. However, when faults (i.e., mutations) are introduced, the output genes deviate from this non-proliferative state. Our study aims to identify the drug or combination of drugs that brings the output genes in the presence of faults as close as possible to the non-proliferative output state. This is determined by comparing the drugged output to the healthy output using the SD score. A higher SD value indicates that the drug fails to suppress the cancerous output genes, whereas an SD value closer to 0 suggests that the drug effectively suppresses them.

For each drug or drug combination, we determined its drugged output across each of the 12383 fault combinations and compared the drugged output to the healthy output to calculate the SD. This resulted in a matrix containing the SD values for each fault across all considered drugs and their combinations.

G. IDENTIFYING ROBUST DRUG COMBINATIONS

After calculating the SD values for each drug combination across all possible fault scenarios, we identified the most effective drug combination for each specific fault by selecting the one with the lowest SD value. To find the drug combination that is the most optimal across all faults, i.e. the drug combination that robustly reduces cell proliferation and maximizes apoptosis, we had to find the mean SD score for a given drug combination. However, comparing the raw average SD scores for various drug combinations is misleading and thus we needed to normalize the raw average SD score for each drug combination with respect to the average SD score for the untreated, i.e. no-drug-applied case. Normalizing with respect to the untreated cases allows us to determine how good the drug combinations are compared to the untreated cases and how they compare against each other. Untreated cases refer to scenarios where the BN circuit has been simulated with the presence of faults and no drug has been applied. We refer to this metric as the Normalized Mean Size Difference (NMSD). Intuitively, the drug combination with the lowest NMSD would be considered the most robust or effective across all possible fault combinations. In Table 4, we present an example matrix of SD for three faults and three drugs. To identify the most effective drug for each specific fault, we select the drug with the lowest SD score. For fault 1, drug 2 demonstrates the lowest SD, indicating it is the most effective in suppressing this fault. Similarly, drug 3 is the optimal choice for fault 2, as it shows the lowest SD for this fault. For fault 3, drug 2 again emerges as the most effective, having the lowest SD among the options. To determine the most effective drug across all three faults, we calculate the NMSD for each drug. This involves normalizing the mean SD relative to the mean SD of the untreated case, as shown in the NMSD column of Table 4. Since drug 2 has the lowest

NMSD, it is the most effective drug across all three faults. The NMSD metric is calculated as follows:

$$NMSD(Drug_i) = \frac{Mean(SD(Drug_i))}{Mean(SD(Untreated))} \quad (3)$$

We calculated the NMSD (Equation 3) for each drug combination in the BN with one, two, and three faults (or mutations) at a time. Given that there are 16 drugs, and we considered up to four drug combinations at a time, this results in a total of 2516 drug combinations. With 12383 combinations of faults, our resulting NMSD matrix would be 2516 (drugs) by 12383 (faults). Presenting and interpreting such a large matrix is impractical, so we have summarized the NMSD scores for each drug combination under one, two, and three mutations (or faults) in the supplementary file (Additional File 1). We simulated the BN and calculated the NMSD using the Python programming language. The code for BN simulation and NMSD table generation is publicly available at the following GitHub repository: <https://github.com/PranabeshTAMU/NSCLC-WithPDL1>.

IV. RESULTS AND DISCUSSION

After simulating the BN model constructed above, we compared the different drug combinations and their efficacy for single, two, and three faults (mutations) at a time, the goal was to identify the most effective combination therapy with the lowest NMSD score. We provided the NMSD scores for each drug combination under one, two, and three mutations (or faults) as tables in the supplementary materials (see Additional File 1). Additionally, each supplemental table (in Additional File 1) includes the top 16 effective drug combinations (i.e., single-drug, two-drug combinations, up to four-drug combinations) for each fault combination. In the following subsections, we discuss some of the topmost effective drug combinations for each fault combination. For the untreated case, the NMSD was equal to 1 (Table 4) which signifies the worst-case scenario, and if the drug combinations showed an NMSD close to 0, it was considered a success. The drug combination that attained the lowest NMSD was the best treatment option (Table 4).

A. DRUG EFFICACY FOR SINGLE DRUG APPLICATION

In our initial Boolean network analysis, we systematically evaluated the efficacy of each drug individually against all possible combinations of single, double, and triple mutations. Figure 4 presents a comprehensive comparison of all 16 drugs' NMSD scores across these mutation scenarios. The NMSD metric quantifies how effectively each drug restores the network towards a non-proliferative state, with lower values indicating better performance. Among all single-drug interventions tested, Capivasertib (an AKT inhibitor) consistently demonstrated superior efficacy, achieving the lowest NMSD score of approximately 0.47 across all mutation scenarios (Tables 5, 6, 7). This represents a substantial 53% improvement compared to the untreated condition, indicating that AKT inhibition alone can significantly counteract the

TABLE 5. Robust drug intervention strategy for single mutation.

Drug Combination	NMSD
Capivasertib	0.473
Trametinib + Capivasertib	0.256
Trametinib + Ribociclib + Capivasertib	0.138
Durvalumab + Trametinib + Ribociclib + Capivasertib	0.078

TABLE 6. Robust drug intervention strategy for two mutations.

Drug Combination	NMSD
Capivasertib	0.478
Ribociclib + Capivasertib	0.294
Durvalumab + Ribociclib + Capivasertib	0.162
Durvalumab + Trametinib + Ribociclib + Capivasertib	0.094

TABLE 7. Robust drug intervention strategy for three mutations.

Drug Combination	NMSD
Capivasertib	0.476
Ribociclib + Capivasertib	0.300
Durvalumab + Ribociclib + Capivasertib	0.169
Durvalumab + Lumakras + Ribociclib + Capivasertib	0.108

effects of multiple oncogenic mutations in NSCLC signaling pathways. Ribociclib, a CDK4/6 inhibitor, showed the second-best performance among single drugs, highlighting the importance of cell cycle regulation in NSCLC treatment (Fig. 4).

B. DRUG EFFICACY FOR TWO DRUG COMBINATIONS

Following the simulation with one drug, the BN model was then simulated with two drug combinations in the simultaneous presence of single, two, and three fault combinations. This simulation tested all two-drug combinations across different fault scenarios, including single-fault, two-fault, and three-fault combinations. Several successful therapeutic outcomes are highlighted in Fig. 5 including some of the best two-drug combinations. The best two-drug combination having the lowest NMSD score for treating NSCLC with a single mutation was Trametinib + Capivasertib (Table 5), which targets MEK and AKT (Table 3). It reduced the NMSD by approximately 74.4% compared to the untreated case. For the two and three mutation cases, the drug combination Ribociclib + Capivasertib (Tables 6, 7) emerged as the most efficacy. Ribociclib is a targeted drug for CDK4/6 (Table 3). This combination demonstrated approximately a 70% reduction in the NMSD score compared to the untreated case.

C. DRUG EFFICACY FOR THREE DRUG COMBINATIONS

Figure 6 displays drug efficacy for three drug cases with a maximum of three faults present at a time among the 42 fault locations. The detailed NMSD values can be found in the supplementary file (Additional File 1), while this paper presents only the top-performing results in Tables 5, 6, 7. Like the preceding subsections, Trametinib + Ribociclib + Capivasertib emerges as the most effective three-drug combination for a

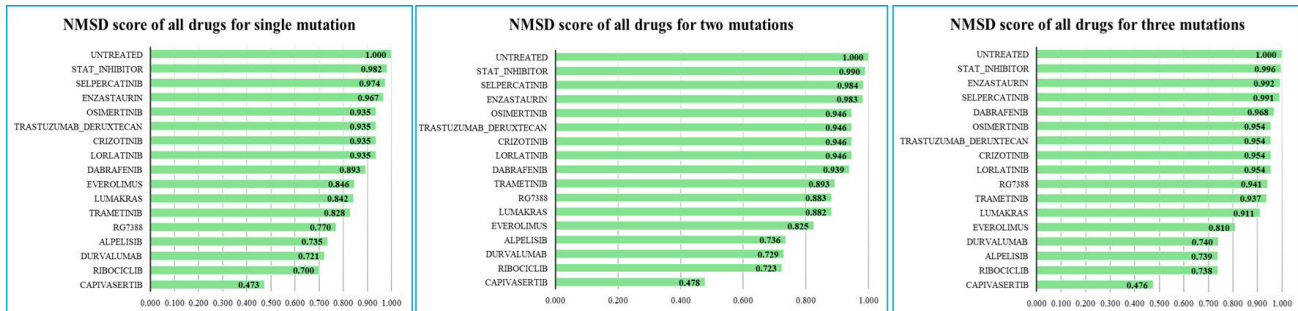


FIGURE 4. All targeted drugs (which are used for this experiment), with respective NMSD scores to treat NSCLC with single, two, and three mutations at a time.

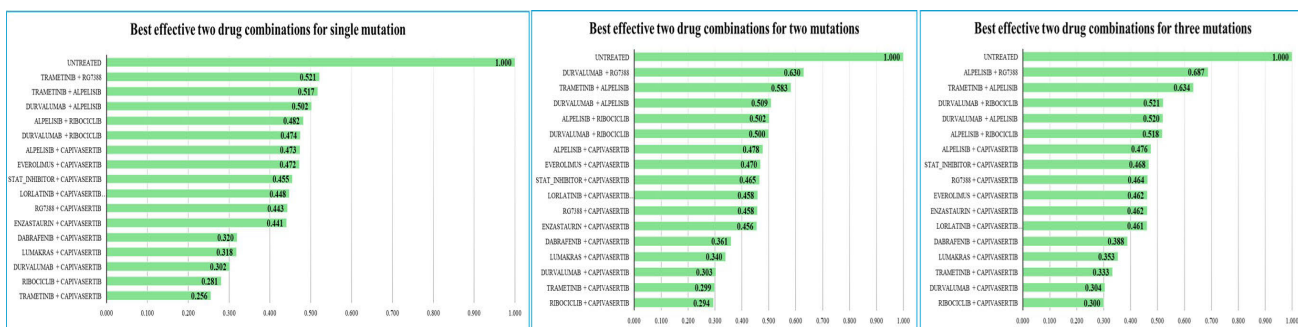


FIGURE 5. Some of the best two drug combinations with the lowest NMSD score to treat NSCLC with single, two, and three mutations at a time.

single mutation scenario, which reduced the NMSD score by 86.2% compared to the untreated case. On the other hand, the drug combination Durvalumab + Ribociclib + Capivasertib held the top position, with the lowest NMSD score, for two and three mutations. The target of Durvalumab was PD-L1 (Table 3). In this case, it is noticeable that all top three drug combinations with the lowest NMSD score, when the number of mutations is high, contained Durvalumab. This combination showed a significant treatment effect in the case of three mutation scenarios with an 83% reduction from the untreated case. Notably, Durvalumab consistently appeared in the top-performing drug combinations across all three-fault scenarios tested, not just in a subset of cases. This remarkable consistency across diverse mutation combinations suggests that the inclusion of PD-L1 inhibition provides robust enhancement of treatment efficacy regardless of the specific mutations present, highlighting the potential universal benefit of incorporating immunotherapy into NSCLC treatment regimens.

D. DRUG EFFICACY FOR FOUR DRUG COMBINATIONS

The best four-drug combination for single and two mutations we found to be Durvalumab + Trametinib + Ribociclib + Capivasertib (Fig. 7), which targets the genes PD-L1+MEK+ CDK4/6 + AKT. Figure 7 presents a comprehensive analysis of the top-performing four-drug combinations across different mutation scenarios in our Boolean network model. The horizontal axis represents the NMSD score, with lower values indicating superior efficacy

in restoring network functionality towards a non-proliferative state. The vertical axis lists the various four-drug combinations tested. Notably, the combination of Durvalumab + Lumakras + Ribociclib + Capivasertib emerges as the most effective regimen for treating networks with three concurrent mutations, achieving an NMSD score of only 0.108 (Table 7). This represents an impressive 89.2% reduction in network disruption compared to the untreated conditions. This particular combination strategically targets four distinct mechanisms: immune checkpoint regulation (PD-L1 inhibition via Durvalumab), KRAS signaling (via Lumakras), cell cycle progression (CDK4/6 inhibition via Ribociclib), and AKT pathway activation (via Capivasertib). The superior performance of this diverse combination highlights the value of simultaneously targeting multiple oncogenic drivers and immune evasion mechanisms in NSCLC with complex mutation profiles. Due to space limitations, all the results are shown in a supplementary file (Additional File 1). We also built a table to display all the parameters used for our experimental design and simulation (Table 8).

E. ANALYSIS AND IMPLICATIONS OF RESULTS

The PI3K/AKT/mTOR pathway is involved in cell growth, proliferation, and survival [65]. Activating mutations within this pathway can lead to uncontrolled cell growth and cancer progression. The AKT inhibitor, Capivasertib, is being investigated in clinical trials for its efficacy in NSCLC [66]. This drug aims to inhibit the activity of the AKT gene,

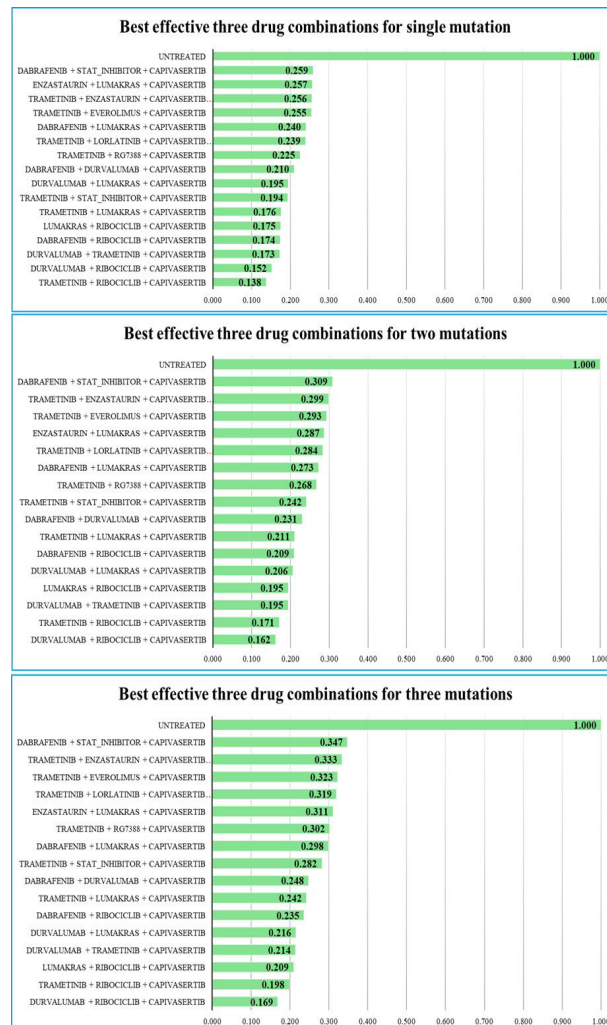


FIGURE 6. Some of the best three-drug combinations with the lowest NMSD score to treat NSCLC with single, two, and three mutations at a time.

thereby slowing down cancer cell growth. CDK4/6 are critical regulators of the cell cycle. Overactivation of these kinases can lead to uncontrolled cell division and tumor growth. The CDK4/6 inhibitor, Ribociclib, is primarily approved for breast cancer but is also being explored for its potential in treating NSCLC [67]; it works by halting the cell cycle, thereby preventing the cancer cells from proliferating. The KRAS pathway is a central regulator of cell growth, metabolism, and survival. Dysregulation of this pathway can contribute to cancer development and progression. The KRAS inhibitor, Lumakras, has been identified for its potential to treat NSCLC [68].

The primary strength of our approach lies in its integration of multiple treatment modalities within a unified computational framework. Unlike previous studies that examined targeted therapies or immunotherapies in isolation, our Boolean network model captures the synergistic interactions between these complementary approaches. This integration enables more accurate prediction of combination therapy effects and provides a theoretical foundation for clinical strategies that

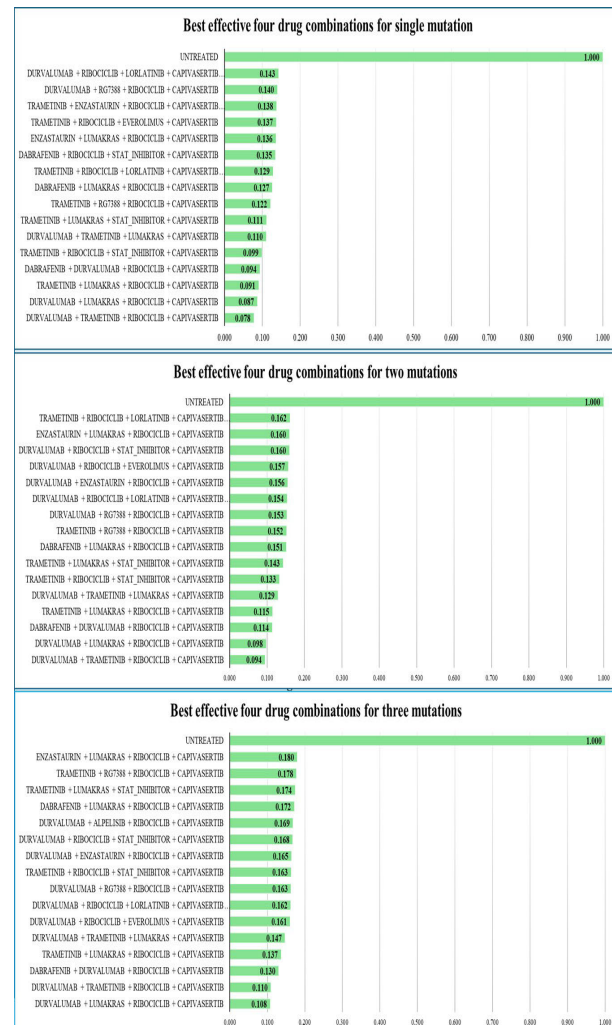


FIGURE 7. Some of the best four-drug combinations with the lowest NMSD score to treat NSCLC with single, two, three, and four mutations at a time.

target both cancer cell-intrinsic oncogenic pathways and tumor-immune interactions simultaneously. Additionally, our model's ability to simulate multiple concurrent mutations more accurately captures the genetic complexity of real NSCLC tumors, which frequently harbor several driver alterations. By restricting our analysis to FDA-approved drugs, we ensure that our predictions have immediate translational potential and could inform the design of clinical trials for novel drug combinations.

In general, our simulations revealed that as the number of mutations in the network increased, the NMSD scores also rose. This makes intuitive sense since an increase in the number of mutations would provide a cancer cell with more avenues to sustain its aberrant signaling, thereby evading the inhibitory effects of the applied drugs. We also observed that while increasing the number of drugs applied does decrease the NMSD score, this strategy becomes less effective with a higher number of mutations. Additionally, administering too many drugs simultaneously to a patient is not a viable strategy, given the associated side effects

TABLE 8. Key parameters of the boolean network model and analysis.

Parameter	Value	Description
Network size	42 nodes	Total number of genes/proteins in the Boolean network
Input nodes	10	Number of input signals to the network
Output nodes	9	Number of reporter genes indicating network state
Maximum mutations	3	Maximum number of concurrent mutations considered
Total mutation combinations	12,383	Total number of mutation scenarios evaluated
Number of drugs	16	Individual drugs considered in the analysis
Maximum drug combination size	4	Maximum number of drugs in a combination
Total drug combinations	2,516	Total number of drug combinations tested
Simulation iterations	31,155,028	Total number of network simulations performed

V. CONCLUSION AND FUTURE WORKS

In this study, we developed a novel computational framework for evaluating combination therapies in NSCLC through Boolean network modeling of integrated oncogenic and immunotherapy pathways. Our model successfully captures the complex interplay between multiple signaling pathways involved in NSCLC progression and predicts the efficacy of various drug combinations in counteracting the effects of genetic mutations.

Our key findings demonstrate that the integration of immunotherapy with targeted therapy substantially enhances treatment efficacy across diverse mutation scenarios. Specifically, combinations including the PD-L1 inhibitor Durvalumab consistently showed superior performance in networks with multiple mutations, providing strong theoretical support for combining immune checkpoint inhibition with targeted pathway inhibition in NSCLC treatment. The optimal four-drug combination identified in our study—Durvalumab + Lumakras + Ribociclib + Capivasertib—targets four distinct mechanisms (immune checkpoint, KRAS signaling, cell cycle progression, and AKT activation), creating a synergistic effect that reduced the normalized mean size difference by 89.2% compared to untreated conditions.

These findings have significant implications for personalized medicine approaches in NSCLC. By predicting how specific drug combinations perform against different mutation profiles, our model could inform treatment selection based on a patient's tumor molecular characteristics. This approach aligns with the growing trend towards precision oncology, where treatments are tailored to the unique genetic makeup of individual tumors.

Immunotherapy, particularly immune checkpoint inhibitors like Durvalumab, has shown remarkable efficacy in treating various cancers by blocking the proteins that prevent T-cells from attacking cancer cells. When combined with targeted therapies that inhibit specific oncogenic proteins (such as

KRAS, AKT, and CDK4/6), there is a synergistic effect. This combination can more effectively suppress cancer growth and prevent the tumor from evading the immune system [69], [70]. One of the major challenges in targeted therapy is the development of drug resistance. Cancer cells often adapt by activating alternative pathways or mutating further. Immunotherapy can help mitigate this issue by providing a robust and adaptive immune response capable of targeting these resistant cancer cells. Targeted therapies focus on specific molecular aberrations, which can limit their efficacy to patients with those mutations. Immunotherapy, however, can induce a broad-spectrum attack on the tumor, recognizing and attacking a wide array of cancer-specific antigens. This makes the combination particularly effective in heterogeneous tumors like NSCLC. Clinical studies have demonstrated that combining immunotherapy with targeted therapy can lead to improved overall survival rates in NSCLC patients [71], [72]. For example, the addition of Durvalumab to a combination therapy regimen has been shown to significantly prolong progression-free survival in patients. The results in this paper provide a firm theoretical basis for these experimental observations. The integration of immunotherapy and targeted therapy fits well within the framework of personalized medicine. By tailoring the treatment to the specific genetic makeup of the tumor and the patient's immune profile, this approach can maximize therapeutic efficacy and minimize adverse effects.

In conclusion, the combination of immunotherapy with targeted therapy offers a promising and multifaceted approach to treating NSCLC. It leverages the strengths of both strategies, providing a more comprehensive attack on cancer while potentially overcoming the limitations associated with each treatment when used alone. As research and clinical trials continue to advance, this combined approach is expected to play an increasingly vital role in the future of NSCLC treatment, ultimately leading to better patient outcomes and prolonged survival.

A significant enhancement to our current model would be the incorporation of additional tumor microenvironment factors that influence the PD-L1/PD-1 axis. We plan to extend our Boolean network to include interactions with various immune cell types, including cytotoxic T cells, regulatory T cells, and myeloid-derived suppressor cells. This extension would provide a more comprehensive representation of the complex interplay between cancer cells and the immune system within the tumor microenvironment. Also including cytokine signaling pathways, particularly those involving IFN- γ , TGF- β , IL-6, and TNF- α —could significantly enhance our model's ability to predict immunotherapy responses. These cytokines play crucial roles in modulating PD-L1 expression, T-cell activation, and immunosuppression. Expanding our Boolean network to incorporate these signaling molecules would create a more comprehensive model of the cancer-immune interface and potentially improve the precision of our drug combination predictions.

Future validation of our computational predictions using *in vitro* NSCLC cell lines (such as A549, H460, and H1299) and patient-derived xenograft models would significantly strengthen our findings. Specifically, examining the combined effects of AKT, KRAS, CDK4/6, and PD-L1 inhibitors on cancer cell viability, apoptosis induction, and immune response activation would provide crucial experimental support for our computational models. A decrease in the expression of these genes would serve as an initial indicator of drug efficacy, warranting further testing on higher-order animal models and eventually progressing to the preclinical trial stage.

Additionally, we aim to explore the mutation landscape in gene regulatory networks and assess its impact on drug development and repurpose, with the overarching goal of enhancing personalized medicine. Understanding the extent to which a mutation or a combination of mutations drives aberrant gene regulatory behavior has significant implications for clinical trial design, including mutation-focused basket-trial formats that are gaining popularity in precision medicine.

Our Boolean network approach offers distinct advantages when compared to alternative computational methods for predicting drug efficacy. Unlike statistical correlation methods that rely solely on empirical data associations, our mechanistic modeling incorporates known biological interactions and causal relationships, providing insights into the underlying mechanisms of drug action. Compared to continuous differential equation models, which require precise kinetic parameters that are often unavailable for complex signaling networks, our Boolean approach captures the essential qualitative behaviors while requiring significantly less parameterization.

Machine learning approaches for drug response prediction can achieve high predictive accuracy but often function as “black boxes” with limited interpretability [73], [74]. In contrast, our Boolean network model provides transparent insights into how specific mutations affect pathway behavior and how drugs modulate these effects. This interpretability is crucial for generating testable hypotheses and guiding experimental validation.

Network-based methods similar to ours have successfully predicted drug combinations for other cancer types [75], [76]. However, our approach is distinguished by its specific integration of immunotherapy with targeted therapy pathways, which is particularly relevant for NSCLC where both treatment modalities have shown clinical efficacy. To the best of our knowledge, this is the first study that integrates multiple oncogenic and immunotherapy signaling pathways into a unified Boolean network framework to simulate drug responses under various mutational conditions in NSCLC. While previous computational studies have focused on individual pathways or limited mutation scenarios, our approach enables a system-level exploration of drug efficacy across diverse mutational landscapes.

In the future, this framework can be extended using probabilistic approaches such as Bayesian networks, especially if sufficient time-series or quantitative expression data become available. Such models may allow for the incorporation of biological variability and uncertainty, enabling even more refined predictions of therapeutic outcomes.

A potential application of the current BN model is in formulating inclusion criteria for basket trials by specifying not only the type but also the number of mutations permitted in the study. Our Boolean network model could directly inform basket trial design for targeted therapies in NSCLC. For example, a basket trial testing the Durvalumab + Capi-vasertib + Ribociclib combination that our model identified as highly effective could stratify patients based on the number and type of mutations in the PI3K/AKT, cell cycle, and immune checkpoint pathways. Based on our computational findings, patients with up to three concurrent mutations in these pathways might be suitable candidates for this combination therapy, while those with more extensive mutational burdens might require alternative approaches. This type of computational guidance could significantly improve patient selection criteria and increase the efficiency of clinical trial design.

Looking forward, we recognize several important directions for enhancing this work:

First, experimental validation using cell lines and animal models is crucial to confirm our computational predictions. Testing the top drug combinations identified in our study on NSCLC cell lines with appropriate genetic backgrounds would provide valuable validation of our theoretical findings.

Second, expanding our model to incorporate the tumor microenvironment would enhance its biological relevance. Including interactions with diverse immune cell populations (T cells, natural killer cells, myeloid cells) and stromal components would create a more comprehensive representation of *in-vivo* tumor dynamics.

Third, integrating pharmacokinetic and pharmacodynamic parameters would improve the clinical applicability of our predictions. Accounting for drug absorption, distribution, metabolism, and excretion could help optimize dosing regimens and sequence for combination therapies.

Fourth, extending our Boolean network to a probabilistic framework would allow for more nuanced modeling of biological variability. This approach could better capture the stochastic nature of cellular responses and provide confidence intervals for our predictions.

Fifth, incorporating resistance mechanisms would address a critical challenge in cancer therapy. Modeling the evolution of treatment resistance over time could help design adaptive treatment strategies that anticipate and prevent the emergence of resistant cell populations.

Finally, developing an interactive software tool based on our model would facilitate its use by clinicians and researchers. Such a tool could allow users to input specific mutation profiles and obtain personalized drug combination

recommendations, bridging the gap between computational prediction and clinical application.

REFERENCES

- [1] World Cancer Research Fund International. (2023). *Lung Cancer Statistics*. Accessed: Oct. 2, 2024. [Online]. Available: <https://www.wcrf.org/cancer-trends/lung-cancer-statistics>
- [2] R. L. Siegel, A. N. Giaquinto, and A. Jemal, "Cancer statistics, 2024," *CA, Cancer J. Clinicians*, vol. 74, no. 1, pp. 12–49, Jan. 2024.
- [3] G. J. Riely et al., "Non-small cell lung cancer, version 4.2024, NCCN clinical practice guidelines in oncology," *J. Nat. Comprehensive Cancer Netw.*, vol. 22, no. 4, pp. 249–274, May 2024.
- [4] M. Araghi, R. Mannani, A. Heidarnejad Maleki, A. Hamidi, S. Rostami, S. H. Safa, F. Faramarzi, S. Khorasani, M. Alimohammadi, S. Tahmasebi, and R. Akhavan-Sigari, "Recent advances in non-small cell lung cancer targeted therapy; An update review," *Cancer Cell Int.*, vol. 23, no. 1, p. 162, Aug. 2023.
- [5] C. Kim and G. Giaccone, "Precision oncology in non-small-cell lung cancer: Opportunities and challenges," *Nature Rev. Clin. Oncol.*, vol. 15, no. 6, pp. 348–349, Jun. 2018.
- [6] *Non-Small Cell Lung Cancer Treatment (PDQ)*, PDQ Adult Treat. Editorial Board, PDQ Cancer Inf. Summaries [Internet]. Nat. Cancer Inst. (U.S.), Bethesda, MD, USA, 2023. Accessed: Mar. 28, 2025. [Online]. Available: <https://www.ncbi.nlm.nih.gov/books/NBK65917/>
- [7] M.-K. Park, J.-M. Lim, J. Jeong, Y. Jang, J.-W. Lee, J.-C. Lee, H. Kim, E. Koh, S.-J. Hwang, H.-G. Kim, and K.-C. Kim, "Deep-learning algorithm and concomitant biomarker identification for NSCLC prediction using multi-omics data integration," *Biomolecules*, vol. 12, no. 12, p. 1839, Dec. 2022.
- [8] Z. Chen, C. M. Fillmore, P. S. Hammerman, C. F. Kim, and K.-K. Wong, "Non-small-cell lung cancers: A heterogeneous set of diseases," *Nature Rev. Cancer*, vol. 14, no. 8, pp. 535–546, Aug. 2014.
- [9] J. K. Sicklick, S. Kato, R. Okamura, M. Schwaeberle, M. E. Hahn, C. B. Williams, P. De, A. Krie, D. E. Piccioni, V. A. Miller, J. S. Ross, A. Benson, J. Webster, P. J. Stephens, J. J. Lee, P. T. Fanta, S. M. Lippman, B. Leyland-Jones, and R. Kurzrock, "Molecular profiling of cancer patients enables personalized combination therapy: The I-PREDICT study," *Nature Med.*, vol. 25, no. 5, pp. 744–750, May 2019.
- [10] M. Wang, R. S. Herbst, and C. Boshoff, "Toward personalized treatment approaches for non-small-cell lung cancer," *Nature Med.*, vol. 27, no. 8, pp. 1345–1356, Aug. 2021.
- [11] J. Minguet, K. H. Smith, and P. Bramlage, "Targeted therapies for treatment of non-small cell lung cancer—Recent advances and future perspectives," *Int. J. Cancer*, vol. 138, no. 11, pp. 2549–2561, Jun. 2016.
- [12] A. C. Tan and D. S. W. Tan, "Targeted therapies for lung cancer patients with oncogenic driver molecular alterations," *J. Clin. Oncol.*, vol. 40, no. 6, pp. 611–625, Feb. 2022.
- [13] L. Horvath, B. Thienpont, L. Zhao, D. Wolf, and A. Pircher, "Overcoming immunotherapy resistance in non-small cell lung cancer (NSCLC)—Novel approaches and future outlook," *Mol. Cancer*, vol. 19, no. 1, pp. 1–5, Dec. 2020.
- [14] P. V. S. Zuniga and D. E. Ost, "Impact of delays in lung cancer treatment on survival," *Chest*, vol. 160, no. 5, pp. 1934–1958, Nov. 2021.
- [15] R. Govindan et al., "Society for immunotherapy of cancer (SITC) clinical practice guideline on immunotherapy for the treatment of lung cancer and mesothelioma," *J. ImmunoTherapy Cancer*, vol. 10, no. 5, May 2022, Art. no. e003956.
- [16] F. A. Shepherd and R. S. Herbst, "Combination strategies to improve immunotherapy in non-small-cell lung cancer," *J. Clin. Oncol.*, vol. 42, no. 5, pp. 417–429, 2024.
- [17] L. W. Elmore, S. F. Greer, E. C. Daniels, C. C. Saxe, M. H. Melner, G. M. Krawiec, W. G. Cance, and W. C. Phelps, "Blueprint for cancer research: Critical gaps and opportunities," *CA, Cancer J. Clinicians*, vol. 71, no. 2, pp. 107–139, Mar. 2021.
- [18] Z.-F. Lim and P. C. Ma, "Emerging insights of tumor heterogeneity and drug resistance mechanisms in lung cancer targeted therapy," *J. Hematol. Oncol.*, vol. 12, no. 1, p. 134, Dec. 2019.
- [19] S. Corso and S. Giordano, "Targeted therapies in cancer and mechanisms of resistance," *J. Mol. Med.*, vol. 92, no. 7, pp. 677–679, Jul. 2014.
- [20] J. Liu, Z. Chen, Y. Li, W. Zhao, J. Wu, and Z. Zhang, "PD-1/PD-L1 checkpoint inhibitors in tumor immunotherapy," *Frontiers Pharmacol.*, vol. 12, Sep. 2021, Art. no. 731798.
- [21] X. Chen, X. Pan, W. Zhang, H. Guo, S. Cheng, Q. He, B. Yang, and L. Ding, "Epigenetic strategies synergize with PD-L1/PD-1 targeted cancer immunotherapies to enhance antitumor responses," *Acta Pharmaceutica Sinica B*, vol. 10, no. 5, pp. 723–733, May 2020.
- [22] H. Vundavilli, A. Datta, C. Sima, J. Hua, R. Lopes, and M. Bittner, "In silico design and experimental validation of combination therapy for pancreatic cancer," *IEEE/ACM Trans. Comput. Biol. Bioinf.*, vol. 17, no. 3, pp. 1010–1018, May 2020.
- [23] P. Bhattacharjee, A. Lahiri, N. P. Reeves, and A. Datta, "Precision targeting of non-small cell lung cancer: Identifying optimal drug targets and FDA-approved combinations for enhanced therapeutic efficacy," in *Proc. IEEE 23rd Int. Conf. Bioinf. Bioeng. (BIBE)*, Dec. 2023, pp. 230–237.
- [24] W. Jing, M. Li, Y. Zhang, F. Teng, A. Han, L. Kong, and H. Zhu, "PD-1/PD-L1 blockades in non-small-cell lung cancer therapy," *OncoTargets Therapy*, p. 489, Jan. 2016.
- [25] National Cancer Institute. *Approved Targeted Therapy Drugs*. Accessed: Aug. 28, 2024. [Online]. Available: <https://www.cancer.gov/about-cancer/treatment/types/targeted-therapies/approved-drug-list>
- [26] U.S. Food and Drug Administration. *Oncology (Cancer) / Hematologic Malignancies Approval Notifications*. Accessed: Aug. 28, 2024. [Online]. Available: <https://www.fda.gov/drugs/resources-information-approved-drugs/oncology-cancer-hematologic-malignancies-approval-notifications>
- [27] National Cancer Institute. *A To Z List of Cancer Drugs*. Accessed: Aug. 28, 2024. [Online]. Available: <https://www.cancer.gov/about-cancer/treatment/drugs>
- [28] R. Saraf, A. Datta, C. Sima, J. Hua, R. Lopes, M. L. Bittner, T. Miller, and H. M. Wilson-Robles, "In silico modeling of the induction of apoptosis by cryptotanshinone in osteosarcoma cell lines," *IEEE/ACM Trans. Comput. Biol. Bioinf.*, vol. 19, no. 3, pp. 1683–1693, May 2022.
- [29] R. S. Saraf, A. Datta, C. Sima, J. Hua, R. Lopes, and M. Bittner, "An in-silico study examining the induction of apoptosis by cryptotanshinone in metastatic melanoma cell lines," *BMC Cancer*, vol. 18, no. 1, pp. 1–3, Dec. 2018.
- [30] J. He, Y. Hu, M. Hu, and B. Li, "Development of PD-1/PD-L1 pathway in tumor immune microenvironment and treatment for non-small cell lung cancer," *Sci. Rep.*, vol. 5, no. 1, p. 13110, Aug. 2015.
- [31] Z. Agur, K. Halevi-Tobias, Y. Kogan, and O. Shlagman, "Employing dynamical computational models for personalizing cancer immunotherapy," *Expert Opinion Biol. Therapy*, vol. 16, no. 11, pp. 1373–1385, Nov. 2016.
- [32] B. Desvergne, L. Michalik, and W. Wahli, "Transcriptional regulation of metabolism," *Physiolog. Rev.*, vol. 86, no. 2, pp. 465–514, 2006.
- [33] R. Sever and J. S. Brugge, "Signal transduction in cancer," *Cold Spring Harb. Perspect. Med.*, vol. 5, no. 4, Apr. 2015, Art. no. a006098.
- [34] Y. Yarden, "The EGFR family and its ligands in human cancer: Signalling mechanisms and therapeutic opportunities," *Eur. J. Cancer*, vol. 37, pp. 3–8, Jan. 2001.
- [35] P. Wee and Z. Wang, "Epidermal growth factor receptor cell proliferation signaling pathways," *Cancers*, vol. 9, no. 5, p. 52, May 2017.
- [36] L. Huang and L. Fu, "Mechanisms of resistance to EGFR tyrosine kinase inhibitors," *Acta Pharmaceutica Sinica B*, vol. 5, no. 5, pp. 390–401, Sep. 2015.
- [37] J.-C. Soria, Y. Ohe, J. Vansteenkiste, T. Reungwetwattana, B. Chewaskulyong, K. H. Lee, A. Dechaphunkul, F. Imamura, N. Nogami, T. Kurata, and I. Okamoto, "Osimertinib in untreated EGFR-mutated advanced non-small-cell lung cancer," *New England J. Med.*, vol. 378, no. 2, pp. 113–125, Jul. 2018.
- [38] R. Roskoski, "The ErbB/HER family of protein-tyrosine kinases and cancer," *Pharmacol. Res.*, vol. 79, no. 1, pp. 34–74, Jan. 2013.
- [39] G. R. R. Ricciardi, A. Russo, T. Franchina, G. Ferraro, M. Zanghì, A. Picone, A. Scimone, and V. Adamo, "NSCLC and HER2: Between lights and shadows," *J. Thoracic Oncol.*, vol. 9, no. 12, pp. 1750–1762, Dec. 2014.
- [40] R. Zandi, A. B. Larsen, P. Andersen, M.-T. Stockhausen, and H. S. Poulsen, "Mechanisms for oncogenic activation of the epidermal growth factor receptor," *Cellular Signalling*, vol. 19, no. 10, pp. 2013–2023, Oct. 2007.
- [41] B. T. Li, E. F. Smit, Y. Goto, K. Nakagawa, H. Udagawa, J. Mazières, M. Nagasaka, L. Bazhenova, A. N. Saltos, E. Felip, and J. M. Pacheco, "Trastuzumab deruxtecan in HER2-mutant non-small-cell lung cancer," *New England J. Med.*, vol. 386, no. 3, pp. 241–251, Jan. 2022.
- [42] B. Hallberg and R. H. Palmer, "Mechanistic insight into ALK receptor tyrosine kinase in human cancer biology," *Nature Rev. Cancer*, vol. 13, no. 10, pp. 685–700, Oct. 2013.

[43] T. Akamine, G. Toyokawa, T. Tagawa, and T. Seto, "Spotlight on lorlatinib and its potential in the treatment of NSCLC: The evidence to date," *OncoTargets Therapy*, vol. 11, pp. 5093–5101, Aug. 2018.

[44] D. Reita, L. Pabst, E. Pencreach, E. Guérin, L. Dano, V. Rimelen, A.-C. Voegeli, L. Vallat, C. Mascaux, and M. Beau-Faller, "Direct targeting KRAS mutation in non-small cell lung cancer: Focus on resistance," *Cancers*, vol. 14, no. 5, p. 1321, Mar. 2022.

[45] E. C. Nakajima, N. Drezner, X. Li, P. S. Mishra-Kalyani, Y. Liu, H. Zhao, Y. Bi, J. Liu, A. Rahman, E. Wearne, I. Ojofeitimi, L. T. Hotaki, D. Spillman, R. Pazdur, J. A. Beaver, and H. Singh, "FDA approval summary: Sotorasib for KRAS G12C-mutated metastatic NSCLC," *Clin. Cancer Res.*, vol. 28, no. 8, pp. 1482–1486, Apr. 2022.

[46] Y. He, M. M. Sun, G. G. Zhang, J. Yang, K. S. Chen, W. W. Xu, and B. Li, "Targeting PI3K/Akt signal transduction for cancer therapy," *Signal Transduction Targeted Therapy*, vol. 6, no. 1, p. 425, Dec. 2021.

[47] Z. Davoodi-Moghaddam, F. Jafari-Raddani, M. Delshad, A. Pourbagheri-Sigaroodi, and D. Bashash, "Inhibitors of the PI3K/AKT/mTOR pathway in human malignancies: trend of current clinical trials," *J. Cancer Res. Clin. Oncol.*, vol. 149, no. 16, pp. 15293–15310, Nov. 2023.

[48] Z. Qureshy, D. E. Johnson, and J. R. Grandis, "Targeting the JAK/STAT pathway in solid tumors," *J. Cancer Metastasis Treatment*, vol. 2020, p. 27, Aug. 2020.

[49] Y. Guo, W. Pan, S. Liu, Z. Shen, Y. Xu, and L. Hu, "ERK/MAPK signalling pathway and tumorigenesis (Review)," *Experim. Therapeutic Med.*, pp. 1997–2007, Jan. 2020.

[50] W. A. Cooper, D. C. Lam, S. A. O'Toole, and J. D. Minna, "Molecular biology of lung cancer," *J. Thoracic Disease*, vol. 5, p. S479, Jan. 2013.

[51] D. Moro-Sibilot et al., "Crizotinib in c-MET- or ROS1-positive NSCLC: Results of the AcSé phase II trial," *Ann. Oncol.*, vol. 30, no. 12, pp. 1985–1991, Dec. 2019.

[52] D. Jurkovicova, C. M. Neophytou, A. Č. Gašparović, and A. C. Gonçalves, "DNA damage response in cancer therapy and resistance: Challenges and opportunities," *Int. J. Mol. Sci.*, vol. 23, no. 23, p. 14672, Nov. 2022.

[53] A. Mogi and H. Kuwano, "TP53 mutations in nonsmall cell lung cancer," *BioMed Res. Int.*, vol. 2011, no. 1, Jan. 2011, Art. no. 583929, doi: [10.1155/2011/583929](https://doi.org/10.1155/2011/583929).

[54] S. Nimmagadda, "Quantifying PD-L1 expression to monitor immune checkpoint therapy: Opportunities and challenges," *Cancers*, vol. 12, no. 11, p. 3173, Oct. 2020.

[55] A. Hartmann, S. Ravichandran, and A. Del Sol, "Modeling cellular differentiation and reprogramming with gene regulatory networks," in *Computational Stem Cell Biology: Methods and Protocols*, vol. 1912. Cham, Switzerland: Springer, 2019, pp. 37–51.

[56] N. Vijesh, S. K. Chakrabarti, and J. Sreekumar, "Modeling of gene regulatory networks: A review," *J. Biomed. Sci. Eng.*, vol. 6, no. 2, pp. 223–231, Feb. 2013.

[57] L. Chen, D. Kulasiri, and S. Samarasinghe, "A novel data-driven Boolean model for genetic regulatory networks," *Frontiers Physiol.*, vol. 9, p. 1328, Sep. 2018.

[58] A. Besozzi, D. Cazzaniga, D. Pescini, and G. Mauri, "A survey of gene regulatory networks modelling methods," *Biophys. Rev.*, vol. 12, no. 2, pp. 123–147, 2020.

[59] H. Lähdesmäki, I. Shmulevich, and O. Yli-Harja, "On learning gene regulatory networks under the Boolean network model," *Mach. Learn.*, vol. 52, nos. 1–2, pp. 147–167, Jul. 2003.

[60] S. A. Kauffman, "Metabolic stability and epigenesis in randomly constructed genetic nets," *J. Theor. Biol.*, vol. 22, no. 3, pp. 437–467, Mar. 1969.

[61] S. Kauffman, "Homeostasis and differentiation in random genetic control networks," *Nature*, vol. 224, no. 5215, pp. 177–178, 1969.

[62] S. Kauffman, "The large scale structure and dynamics of gene control circuits," *J. Theor. Biol.*, vol. 44, no. 1, pp. 167–190, Mar. 1974.

[63] P. Trairatphisan, A. Mizra, J. Pang, A. A. Tantar, J. Schneider, and T. Sauter, "Recent development and biomedical applications of probabilistic Boolean networks," *Cell Commun. Signaling*, vol. 11, no. 1, p. 46, 2013.

[64] A. Lahiri, H. Vundavilli, M. Mondal, P. Bhattacharjee, B. Decker, G. D. Priore, N. P. Reeves, and A. Datta, "Drug target identification in triple negative breast cancer stem cell pathways: A computational study of gene regulatory pathways using Boolean networks," *IEEE Access*, vol. 11, pp. 56672–56690, 2023.

[65] H. Cheng, M. Shcherba, G. Pendurthi, Y. Liang, B. Piperdi, and R. Perez-Soler, "Targeting the PI3K/AKT/mTOR pathway: Potential for lung cancer treatment," *Lung Cancer Manage.*, vol. 3, no. 1, pp. 67–75, Feb. 2014.

[66] DrugBank. *Capivasertib Completed Phase 2 Trials for Metastatic Non-Small Cell Lung Cancer*. Accessed: Jan. 13, 2025. [Online]. Available: https://go.drugbank.com/drugs/DB12218/clinical_trials?conditions=DBCOND0043377&phase=2&purpose=treatment&status=completed

[67] C. L. Braal, E. M. Jongbloed, S. M. Wilting, R. H. J. Mathijssen, S. L. W. Koolen, and A. Jager, "Inhibiting CDK4/6 in breast cancer with palbociclib, ribociclib, and abemaciclib: Similarities and differences," *Drugs*, vol. 81, no. 3, pp. 317–331, Feb. 2021.

[68] É. O'Sullivan, A. Keogh, B. Henderson, S. P. Finn, S. G. Gray, and K. Gately, "Treatment strategies for KRAS-mutated non-small-cell lung cancer," *Cancers*, vol. 15, no. 6, p. 1635, Mar. 2023.

[69] W.-J. Liu, Y. Du, R. Wen, M. Yang, and J. Xu, "Drug resistance to targeted therapeutic strategies in non-small cell lung cancer," *Pharmacol. Therapeutics*, vol. 206, Feb. 2020, Art. no. 107438.

[70] E. Shtivelman, T. Hensing, G. R. Simon, P. A. Dennis, G. A. Otterson, R. Bueno, and R. Salgia, "Molecular pathways and therapeutic targets in lung cancer," *Oncotarget*, vol. 5, no. 6, pp. 1392–1433, Mar. 2014.

[71] C. Rolfo, C. Caglevic, M. Santarpia, A. Araujo, E. Giovannetti, C. D. Gallardo, P. Pauwels, and M. Mahave, "Immunotherapy in NSCLC: A promising and revolutionary weapon," *Immunotherapy*, vol. 995, pp. 97–125, Jan. 2017.

[72] C. Manegold et al., "The potential of combined immunotherapy and antiangiogenesis for the synergistic treatment of advanced NSCLC," *J. Thoracic Oncol.*, vol. 12, no. 2, pp. 194–207, Feb. 2017.

[73] P. Geeleher, N. J. Cox, and R. S. Huang, "Clinical drug response can be predicted using baseline gene expression levels and in vitro drug sensitivity in cell lines," *Genome Biol.*, vol. 15, no. 3, p. 47, Mar. 2014.

[74] T. Sakellaropoulos et al., "A deep learning framework for predicting response to therapy in cancer," *Cell Rep.*, vol. 29, no. 11, pp. 3367–3373.e4, 2019.

[75] Å. Fløbak, A. Baudot, E. Remy, L. Thommesen, D. Thieffry, M. Kuiper, and A. Lægreid, "Discovery of drug synergies in gastric cancer cells predicted by logical modeling," *PLOS Comput. Biol.*, vol. 11, no. 8, Aug. 2015, Art. no. e1004426.

[76] D. Silverbush and R. Sharan, "Network-based prediction of drug combinations," *Sci. Rep.*, vol. 7, p. 9237, Jan. 2017.



PRANABESH BHATTACHARJEE received the M.Tech. degree in VLSI design and microelectronics technology from Jadavpur University, Kolkata, India, in 2019. He is currently pursuing the Ph.D. degree with the Genomic Signal Processing Laboratory, Department of Electrical and Computer Engineering, Texas A&M University, College Station, TX, USA. He has over six years of professional experience in industry and academic. Before joining the Ph.D. degree, he was a Research Fellow with the University of Engineering and Management Kolkata, India, under the DST-SERB (Government of India) Project. He has two journals and two international conference publications to date. He is also working on an NSF-funded cancer research project focused on protein target-based drug discovery for cancer treatment.



ADITYA LAHIRI received the B.S. degree in electrical engineering from Purdue University, West Lafayette, IN, USA, in 2016, and the M.S. and Ph.D. degrees in electrical engineering from Texas A&M University, College Station, TX, USA, in 2018 and 2022, respectively. His research interests include bioinformatics, machine learning, and graph theory applied to drug and target discovery in pediatric cancers.



TANMAY SINDHWANI is currently pursuing the bachelor's degree in electrical engineering with Texas A&M University, College Station, TX, USA. With a keen interest in robotics and engineering, he has been a part of various organizations on campus, such as TAMU Robomasters and Aggies Create, gaining essential real-time problem-solving skills. He is currently a Research Assistant with the Department of Electrical and Computer Engineering on several different genomic and bioelectronic projects.



ANIRUDDHA DATTA (Fellow, IEEE) received the B.Tech. degree in electrical engineering from the Indian Institute of Technology Kharagpur, Kharagpur, India, in 1985, the M.S.E.E. degree from Southern Illinois University, Carbondale, IL, USA, in 1987, and the M.S. degree in applied mathematics and the Ph.D. degree from the University of Southern California, Los Angeles, CA, USA, in 1991. In August 1991, he joined the Department of Electrical and Computer Engineering, Texas A&M University, where he is currently the J. W. Runyon, Jr. '35 Professor II and the Co-Director of Graduate Programs. His research interests include adaptive control, robust control, PID control, and genomic signal processing. He has authored or co-authored five books and more than 200 journals and conference papers on these topics. He has served as an Associate Editor for IEEE TRANSACTIONS ON AUTOMATIC CONTROL, from 2001 to 2003, IEEE TRANSACTIONS ON SYSTEMS, MAN AND CYBERNETICS—PART B: CYBERNETICS, from 2005 to 2006, IEEE TRANSACTIONS ON BIOMEDICAL ENGINEERING, from 2013 to 2015, EURASIP *Journal on Bioinformatics and Systems Biology*, from 2007 to 2016, IEEE JOURNAL OF BIOMEDICAL AND HEALTH INFORMATICS, from 2014 to 2016, IEEE/ACM TRANSACTIONS ON COMPUTATIONAL BIOLOGY AND BIOINFORMATICS, from 2014 to 2017, and IEEE ACCESS, from 2013 to 2022. He is also serving as an Academic Editor for *PLOS One*.



NORMAN PETER REEVES received the Ph.D. degree in biomedical engineering from Yale University, in 2007. He is currently the Founder and the President of Sumaq Life LLC, a life science company. Sumaq Life LLC was formed to create health-related technological innovations and increase the translation of scientific discoveries into real-world applications. Before Sumaq Life LLC, he was a Research Associate Professor with the College of Osteopathic Medicine, Michigan State University, specializing in orthopedic research and biological modeling. He has authored/co-authored more than 60 peer-reviewed publications and has been a PI/Co-PI on U.S. \$5M in federally funded research. He was a recipient of the 2005 International Society for the Study of the Lumbar Spine (ISSLS) Basic Research Award and the 2008 Rose Excellence in Research Award for Orthopedic Physical Therapy Research.